AIAA JOURNAL
Vol. 32, No. 10, October 1994

Three-Dimensional Elasticity Solutions to Vibration of Cantilevered Skewed Trapezoids

K. M. Liew,* K. C. Hung,† and M. K. Lim‡
Nanyang Technological University, 2263 Singapore

An accurate three-dimensional elasticity model for determining the free vibration response of skewed trapezoidal plates is presented. The method is formulated on the basis of a linear, small-strain, three-dimensional elasticity theory with the Ritz minimization procedure. The solution method uses sets of uniquely defined one- and two-dimensional polynomial functions to approximate the trial displacements in the thickness and surface directions, respectively. These functions are orthogonally generated and have been proven to be highly efficient and numerically stable. The proposed technique yields natural frequencies and mode shapes for a wide range of cantilevered skewed trapezoidal plates of arbitrary planform. The accuracy of these results, whenever possible, is validated through comparison with the analytical and experimental data. Parametric investigations on the vibration behavior of cantilevered trapezoidal plates with respect to different thickness ratios, skew angles, and chord ratios have been carried out. For the first time, the presence of surface parallel symmetric thickness modes for these plates is demonstrated in vivid three-dimensional mode shape plots.

I. Introduction

DESPITE the practical importance of skewed trapezoidal plates in numerous engineering applications, theoretical research on the free vibration of these structures is very recent and the accumulated data are extremely limited. Most of the researchers in this field have followed the classical thin plate formulation, which inevitably restricts the scope of analysis to thin skewed trapezoidal plates.[1–3] For thin plates, the complicating effects of transverse shear deformation and rotary inertia can be neglected. For moderately thick or very thick plates, however, formulations based on the thin plate theory tend to overestimate the dynamic stiffness of these structures and lead to inaccurate results.

Attempts have been made in recent years, notably by Kitipornchai et al.,[4,5] to compensate for this drawback in classical thin plate theory. In their works, the Mindlin first-order shear deformable plate theory was used.[6] With the appropriate choice of the shear correction factor κ, they were able to predict a wide range of natural frequencies for triangular and trapezoidal plates of moderate thickness. The Mindlin formulation, however, is incapable of predicting a full vibration spectrum for thick structures. Srinivas et al.[7] in their classical paper reported on the vibrations of simply supported rectangular plates based on the exact three-dimensional elasticity theory. They have pointed out that, to obtain a complete dynamic characterization of thick plates, three-dimensional elasticity theory must be employed. A recent study by Liew et al.[8] expounded further on the three-dimensional free vibration of thick rectangular plates. A comprehensive set of frequency results and mode shapes were presented for plates with different boundary constraints. In the three-dimensional elasticity approach, the complicating effects due to the thickness shear variation are implicitly accounted for. In addition, for plates having acute skew geometries, the three-dimensional formulation has the added advantage of inherently eliminating the numerical difficulties associated with the stress singularity at the skew edges.

This paper presents a global three-dimensional Ritz formulation for the vibration analysis of cantilevered skewed trapezoidal plates. The method is based on the exact linear, small-strain, three-dimensional elasticity theory in conjunction with the Ritz minimum energy principle. The solution process uses sets of one- and two-dimensional polynomial functions to approximate, respectively, the thickness and the surface variations of the spatial displacement fields. These functions are orthogonally generated and have been proven to be highly efficient and stable in many numerical applications.[9,10]

The primary objective of this study is to apply the three-dimensional Ritz method to the vibrations of cantilevered skewed trapezoidal plates of different planforms. The validity of the numerical procedure is established through extensive convergence tests and comparison with the existing analytical and experimental results. In this paper, the relative effects of each geometric parameter on the fundamental and higher frequencies are discussed. Detailed

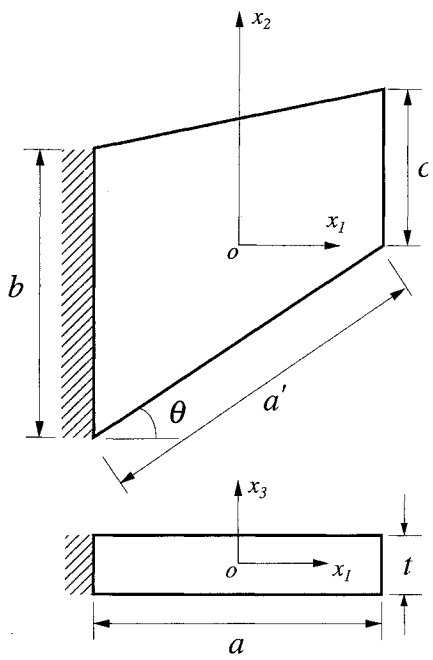

Fig. 1 Geometry of the cantilevered skewed trapezoidal plate.

Received July 21, 1993; revision received Jan. 24, 1994; accepted for publication Jan. 24, 1994.

*Director, Dynamics and Vibration Center, School of Mechanical and Production Engineering, Nanyang Avenue.

†Research Assistant, Dynamics and Vibration Center, School of Mechanical and Production Engineering, Nanyang Avenue.

‡Associate Professor and Dean of School of Mechanical and Production Engineering, Nanyang Avenue.

Table 1 Convergence of frequency parameters $\bar{\lambda} = (\omega b^2/2\pi)(\rho t/D)^{1/2}$ for cantilevered skewed trapezoidal plates with $\nu = 0.3$

Thickness ratio t/b	Terms $p \times q$	Mode sequence number 1	2	3	4	5	6
a) Triangular plate with $a/b = \sqrt{3/2}$ and $\theta = 30$ deg							
0.01	5 × 3	1.4302	5.6601	6.1701	15.331	15.910	18.380
	7 × 4	1.4240	5.5965	6.1371	14.281	14.832	17.167
	10 × 5	1.4222	5.5869	6.1283	14.258	14.806	17.136
	11 × 5	1.4215	5.5836	6.1250	14.250	14.796	17.125
	12 × 5	1.4210	5.5810	6.1224	14.243	14.788	17.116
	13 × 5	1.4208	5.5798	6.1218	14.240	14.783	17.111
	5 × 3	1.3877	5.0635	5.6045	7.0598	12.390	12.523
	7 × 4	1.3822	5.0289	5.5755	7.0553	12.106	12.217
0.10	10 × 5	1.3811	5.0249	5.5712	7.0545	12.093	12.206
	11 × 5	1.3808	5.0239	5.5700	7.0543	12.091	12.204
	12 × 5	1.3806	5.0231	5.5692	7.0541	12.089	12.202
b) Trapezoidal plate with $a/b = 1.0$, $c/b = 0.6$, and $\theta = \tan^{-1}(1/5)$							
0.01	5 × 3	0.6419	2.0814	3.6008	6.3901	8.0794	10.032
	7 × 4	0.6373	2.0583	3.5690	6.2027	7.8096	9.6455
	10 × 5	0.6363	2.0540	3.5632	6.1889	7.8014	9.6202
	11 × 5	0.6360	2.0524	3.5614	6.1844	7.7992	9.6141
	12 × 5	0.6358	2.0515	3.5600	6.1804	7.7964	9.6102
	13 × 5	0.6356	2.0510	3.5596	6.1789	7.7958	9.6091
	5 × 3	0.6324	1.9470	3.4010	3.9638	5.7065	7.1818
	7 × 4	0.6294	1.9295	3.3762	3.9541	5.5843	7.1023
0.10	10 × 5	0.6288	1.9270	3.3726	3.9523	5.5760	7.0965
	11 × 5	0.6286	1.9265	3.3717	3.9518	5.5742	7.0955
	12 × 5	0.6285	1.9261	3.3710	3.9515	5.5730	7.0946

Table 2 Comparison of $\bar{\lambda} = (\omega b^2/2\pi)(\rho t/D)^{1/2}$ for cantilevered skewed trapezoidal plates with $\nu = 0.3$ and $t/b = 0.01$

θ, deg	Side ratio a'/b	Reference	Mode sequence number 1	2	3	4	5	6
a) Skewed triangular plate with $c/b = 0.0$								
0	1.0	Mirza and Bijlani[1]	0.980	3.670	5.298	8.899	11.855	15.831
		McGee et al.[3]	0.9808	3.7332	5.1966	8.9366	12.164	—
		Gustafson et al.[12]	0.9237	3.642	5.088	8.703	11.81	—
		Present	0.9819	3.7330	5.1934	8.9253	12.146	15.763
	2.0	Mirza and Bijlani[1]	0.267	1.174	2.029	3.094	4.885	6.676
		Present	0.2638	1.1327	1.9642	2.7735	4.6440	5.2882
−30	1.0	Mirza and Bijlani[1]	0.917	3.358	5.722	8.617	10.730	16.373
		McGee et al.[3]	0.9054	3.414	5.7167	8.6574	11.165	—
		Present	0.9071	3.4175	5.7191	8.6404	11.156	16.274
	2.0	Mirza and Bijlani[1]	0.251	1.072	2.169	3.047	4.655	6.544
		Present	0.2445	1.0278	2.1253	2.7333	4.2399	5.6524
b) Skewed trapezoidal plate with $c/b = 0.5$								
0	1.0	McGee et al.[3]	0.6469	2.2643	3.5784	6.2806	9.3199	—
		Present	0.6480	2.2630	3.5824	6.2751	9.3120	9.6922
	2.0	McGee et al.[3]	0.1648	0.8879	1.0201	2.3798	2.7111	—
		Present	0.1651	0.8892	1.0197	2.3825	2.7102	4.5275
−30	1.0	McGee et al.[3]	0.6512	2.2854	4.1204	5.6488	9.7150	—
		Present	0.6529	2.2877	4.1310	5.6466	9.7061	10.947
	2.0	McGee et al.[3]	0.1629	0.8264	1.2487	2.1434	3.2753	—
		Present	0.1635	0.8287	1.2554	2.1472	3.2903	4.0047

three-dimensional mode shapes are presented for selected cases to enhance our understanding of the physics of plate vibrations.

II. Theoretical Formulation

A. Preliminary Definition

For a thick skewed trapezoidal plate undergoing small-amplitude vibration, the spatial displacement at a general point may be resolved into u_1, u_2 (in-plane motion) and u_3 (out-of-plane motion) components, respectively. The plate is defined in a right-handed orthogonal coordinate system (x_1, x_2, x_3), with the top and bottom surfaces of the plate parallel to the reference plane containing x_1 and x_2 as shown in Fig. 1. The aspect ratio a/b is defined as the ratio of the spanwise dimension to the chordwise dimension at the root of the plate. The chord ratio c/b is defined as the ratio of the chord length at the tip to the chord length at the clamped end. The parameter t/b is defined to be the thickness ratio. The angle θ, which measures positive in the clockwise direction, is the degree of skewness of the trapezoids.

B. Formulation of Energy Functional

With $\varepsilon = \{\varepsilon_{ij}\}$, $i, j = 1, 2, 3$, and $\sigma = \{\sigma_{ij}\}$, $i, j = 1, 2, 3$, denoting the strain and stress tensors, respectively, we can express the strain energy of the plate in the following form:

$$V = \frac{1}{2}\iiint_v \sigma^T \varepsilon \, dv \tag{1}$$

with the integration performed over the total volume of the plate.

The constitutive relation between the stress and strain is given by

$$\sigma = \boldsymbol{D}\varepsilon \tag{2}$$

in which $\boldsymbol{D}$ is the compliance matrix. For a three-dimensional transversely isotropic elastic body, Hooke's law, Eq. (2), can be written in full as

Table 3 Comparison of $\bar{\lambda} = (\omega b^2/2\pi)(\rho t/D)^{1/2}$ for cantilevered isosceles triangular plates $c/b = 0.0$, $a/b = 1/(2 \tan \theta)$, and $\nu = 0.3$

θ, deg	Thickness t/b	Reference	Mode sequence number 1	2	3	4	5	6
15	≤ 0.01	Kitipornchai et al.[4]	0.3144	1.3615	2.1413	3.3119	5.3142	6.1280
		Present	0.3149	1.3645	2.1405	3.3157	5.3093	6.1323
	0.10	Kitipornchai et al.[4]	0.3115	1.3257	1.9796	3.1477	4.7253	5.6466
		Present[a]	0.3121	1.3293	1.9852	3.1584	4.7424	5.6712
30	≤ 0.01	Bhat[2]	1.4200	5.5915	6.1283	14.418	14.885	17.521
		Kitipornchai et al.[4]	1.4197	5.5847	6.1246	14.261	14.823	17.154
		Present	1.4210	5.5810	6.1224	14.243	14.788	17.116
	0.10	Kitipornchai et al.[4]	1.3758	4.9994	5.5399	12.004	12.120	13.852
		Present[b]	1.3806	5.0231	5.5692	12.089	12.202	13.966
45	≤ 0.01	Kitipornchai et al.[4]	4.0250	11.438	16.847	26.816	30.524	41.879
		Present	4.0259	11.428	16.796	26.752	30.385	41.571
	0.10	Kitipornchai et al.[4]	3.7410	9.6608	13.410	20.105	22.190	27.956
		Present[c]	3.7620	9.7337	13.530	20.326	22.420	28.309

[a]Additional modes predicted in the three-dimenstional Ritz method are 2.0568 and 4.9996.
[b]Additional modes predicted in the three-dimenstional Ritz method are 7.0541 and 13.772.
[c]Additional modes predicted in the three-dimenstional Ritz method are 13.996, 22.400, and 25.423.

Table 4 Comparison of $\bar{\lambda} = (\omega b^2/2\pi)(\rho t/D)^{1/2}$ for cantilevered symmetric trapezoidal plates with $\nu = 0.3$

Aspect ratio c/b	a/b	Thickness t/b	Reference	Mode sequence number 1	2	3	4	5	6
0.2	1.0	≤ 0.01	Kitipornchai et al.[5]	0.8194	3.5255	3.8817	9.1797	9.8442	12.532
			Present	0.8207	3.5248	3.8858	9.1710	9.8488	12.525
		0.10	Kitipornchai et al.[5]	0.8042	3.2300	3.6363	7.9537	8.6828	10.671
			Present[a]	0.8064	3.2397	3.6531	7.9862	8.7282	10.727
	2.0	≤ 0.01	Kitipornchai et al.[5]	0.2079	0.9840	1.5190	2.5253	3.7186	4.8212
			Present	0.2076	0.9856	1.5192	2.5294	3.7169	4.8279
		0.10	Kitipornchai et al.[5]	0.2059	0.9652	1.4170	2.4294	3.3815	4.5179
			Present[b]	0.2063	0.9674	1.4199	2.4363	3.3899	4.5339
0.6	1.0	≤ 0.01	Kitipornchai et al.[5]	0.6345	2.0513	3.5556	6.1859	7.8021	9.6070
			Present	0.6358	2.0515	3.5600	6.1804	7.7964	9.6102
		0.10	Kitipornchai et al.[5]	0.6267	1.9216	3.3580	5.5534	7.0738	8.4958
			Present[c]	0.6285	1.9261	3.3710	5.5730	7.0946	8.5408
	2.0	≤ 0.01	Kitipornchai et al.[5]	0.1535	0.8918	0.8927	2.4306	2.4697	4.4882
			Present	0.1588	0.8933	0.8941	2.4352	2.4699	4.4896
		0.10	Kitipornchai et al.[5]	0.1577	0.8470	0.8774	2.3141	2.3438	4.1354
			Present[d]	0.1580	0.8485	0.8795	2.3191	2.3507	4.1473

[a]Additional modes predicted in the three-dimenstional Ritz method are 4.7385 and 10.517.
[b]Additional modes predicted in the three-dimenstional Ritz method are 1.4764 and 4.3000.
[c]Additional mode predicted in the three-dimenstional Ritz method is 3.9515.
[d]Additional mode predicted in the three-dimenstional Ritz method is 1.2583.

$$\begin{Bmatrix} \sigma_{11} \\ \sigma_{22} \\ \sigma_{33} \\ \sigma_{12} \\ \sigma_{23} \\ \sigma_{13} \end{Bmatrix} = \begin{bmatrix} d_{11} & d_{12} & d_{13} & 0 & 0 & 0 \\ & d_{22} & d_{23} & 0 & 0 & 0 \\ & & d_{33} & 0 & 0 & 0 \\ & & & d_{44} & 0 & 0 \\ & \text{sym} & & & d_{55} & 0 \\ & & & & & d_{66} \end{bmatrix} \begin{Bmatrix} \varepsilon_{11} \\ \varepsilon_{22} \\ \varepsilon_{33} \\ \varepsilon_{12} \\ \varepsilon_{23} \\ \varepsilon_{13} \end{Bmatrix} \tag{3}$$

where σ_{ij}, $i = 1, 2, 3$, are the normal stresses, and σ_{12}, σ_{23}, and σ_{13} are the shear stresses. On the right-hand side of the equation, ε_{ij} are the corresponding strain components. For isotropic materials, the components d_{ij} are given by

$$d_{ii} = \lambda + 2G, \qquad i = 1, 2, 3 \tag{4a}$$

$$d_{12} = d_{13} = d_{23} = \lambda \tag{4b}$$

$$d_{ii} = 2G, \qquad i = 4, 5, 6 \tag{4c}$$

The Lamé constants λ and G (shear modulus) are defined as

$$\lambda = \frac{\nu E}{[(1+\nu)(1-2\nu)]} \tag{5a}$$

$$G = \frac{E}{2(1+\nu)} \tag{5b}$$

where E is the modulus of elasticity and ν is the Poisson ratio.

The linear strain components at a general point can be defined in terms of the spatial displacement quantities

$$\varepsilon_{ii} = \frac{\partial u_i}{\partial x_i}, \qquad i = 1, 2, 3 \tag{6a}$$

$$\varepsilon_{1i} = \frac{\partial u_1}{\partial x_i} + \frac{\partial u_i}{\partial x_1}, \qquad i = 2, 3 \tag{6b}$$

$$\varepsilon_{23} = \frac{\partial u_2}{\partial x_3} + \frac{\partial u_3}{\partial x_2} \tag{6c}$$

Inserting Eqs. (2–6) into the strain energy expression defined in Eq. (1) and expanding yields

$$V = \frac{1}{2}\iiint_v \left\{ \lambda \left(\sum_{i=1}^{3} u_{i,i} \right)^2 + 2G \left(\sum_{i=1}^{3} u_{i,i}^2 \right) + G\left[(u_{1,2} + u_{2,1})^2 + (u_{2,3} + u_{3,2})^2 + (u_{1,3} + u_{3,1})^2 \right] \right\} dv \tag{7}$$

The comma convention is applied to denote partial differentiation.

Similarly, the kinetic energy of the plate can be expressed as

$$T = \frac{\rho}{2}\iiint_V \sum_{i=1}^{3} \dot{u}_i^2 \, dv \tag{8}$$

in which ρ is the mass per unit volume, and $\dot{u}_i$, $i = 1, 2, 3$, are the velocity components in each direction. For simple harmonic motion, the periodic displacement components can be expressed in terms of the displacement amplitude functions,

$$u_i = U_i(x_1, x_2, x_3)\, e^{i\omega t}; \quad i = 1, 2, 3 \tag{9}$$

Finally we defined a total energy functional of the form

$$\Pi = V_{max} - T_{max} \tag{10}$$

where V_{max} and T_{max} are the maximum strain and kinetic energies of the plate in a vibratory cycle, respectively. They are obtained from Eqs. (7–9) by eliminating the periodic elements and replacing the displacement components by the corresponding amplitude functions.

The displacement amplitude functions are assumed in the form of double series polynomials

$$U_i = \sum_{m=1}^{M}\sum_{n=1}^{N} C_{mn}^{i}\, {}^{i}\phi_m(x_1, x_2)\, {}^{i}\psi_n(x_3), \quad i = 1, 2, 3 \tag{11}$$

In the preceding expression, ${}^{i}\psi_n(x_3)$ are the one-dimensional polynomial approximations across the plate thickness; ${}^{i}\phi_m(x_1, x_2)$, on the other hand, are the two-dimensional polynomial functions used to approximate the surface variation of the plate, and C_{mn}^{i} are the undetermined coefficients of the respective amplitude functions. The method of construction and the characteristics of these polynomial functions will be discussed in the following section.

III. Method of Solution

A. Variable-Order Polynomial-Based Displacement Functions

The set of one-dimensional thickness function ${}^{i}\psi_n(x_3)$ is constructed from the following recurrence relation[11]:

$$\begin{aligned} {}^{i}\psi_{k+1}(x_3) &= [g(x_3) - B_k]\,[{}^{i}\psi_k(x_3)] \\ &\quad - C_k[{}^{i}\psi_{k-1}(x_3)]; \quad k = 1, 2, \ldots \end{aligned} \tag{12}$$

where

$$B_k = \frac{\int_{-t/2}^{t/2} g(x_3)\,[{}^{i}\psi_k^2(x_3)]\, dx_3}{\int_{-t/2}^{t/2} {}^{i}\psi_k^2(x_3)\, dx_3} \tag{13a}$$

and

$$C_k = \frac{\int_{-t/2}^{t/2} [{}^{i}\psi_k^2(x_3)]\, dx_3}{\int_{-t/2}^{t/2} {}^{i}\psi_{k-1}^2(x_3)\, dx_3} \tag{13b}$$

The polynomial ${}^{i}\psi_0(x_3)$ is defined as zero, and the basic function ${}^{i}\psi_1(x_3)$ is chosen to take advantage of the symmetry of the plate in the thickness direction. For symmetric thickness modes, in which the in-plane displacements u_1 and u_2 are each even function of the one-dimensional polynomials, the basic functions ${}^{i}\psi_1(x_3)$ and the corresponding generating functions $g(x_3)$ have the following forms:

$${}^{i}\psi_1(x_3) = 1.0 \text{ and } g(x_3) = x_3^2; \quad i = 1, 2 \tag{14a}$$

$${}^{3}\psi_1(x_3) = x_3 \text{ and } g(x_3) = x_3^2 \tag{14b}$$

For antisymmetric thickness modes with the in-plane displacements u_1 and u_2 each odd function of the one-dimensional polynomials, the basic functions ${}^{i}\psi_1(x_3)$ for each displacement component are chosen as

$${}^{i}\psi_1(x_3) = x_3 \text{ and } g(x_3) = x_3^2; \quad i = 1, 2 \tag{15a}$$

$${}^{3}\psi_1(x_3) = 1.0 \text{ and } g(x_3) = x_3^2 \tag{15b}$$

These sets of thickness variation functions collectively satisfy the stress free boundary conditions at the top and bottom surfaces of the plate. In addition, these functions follow the orthogonality relation

$$\int_{-t/2}^{t/2} [{}^{i}\psi_j(x_3)]\,[{}^{i}\psi_k(x_3)]\, dx_3 = \delta_{jk} \tag{16}$$

where δ_{jk} is the Kronecker delta function.

The sets of two-dimensional surface functions ${}^{i}\phi_m(x_1, x_2)$, on the other hand, are constructed as follows[10]:

$${}^{i}\phi_j(x_1, x_2) = f_j(x_1, x_2)[{}^{i}\phi_1(x_1, x_2)] - \sum_{k=1}^{j-1} {}^{i}\Xi_{jk}\,[{}^{i}\phi_k(x_1, x_2)] \tag{17}$$

in which

$${}^{i}\Xi_{jk} = \frac{\iint_A f_j(x_1, x_2)\,[{}^{i}\phi_1(x_1, x_2)]\,[{}^{i}\phi_k(x_1, x_2)]\, dx_1\, dx_2}{\iint_A [{}^{i}\phi_k^2(x_1, x_2)]\, dx_1\, dx_2} \tag{18}$$

The index $i = 1, 2, 3$ denotes the respective displacement direction.

In the preceding expression,

$$\sum_{j=1}^{m} f_j(x_1, x_2) = \sum_{q=0}^{p}\sum_{i=0}^{q} x_1^{q-i} x_2^{i} \tag{19}$$

is a mathematically complete set of two-dimensional polynomial space of order p. The number of terms m is related to p by

$$m = \frac{(p+1)(p+2)}{2} \tag{20}$$

The essential geometric boundary conditions of the skewed trapezoidal plate are uniquely characterized by the choice of the basic functions ${}^{i}\phi_1(x_1, x_2)$. In this study, the plate is assumed to be fully clamped on an edge, whereas the remaining edges are stress free. The corresponding boundary conditions are

$$u_1 = u_2 = u_3 = 0, \text{ at } x_1 = -a/2 \tag{21}$$

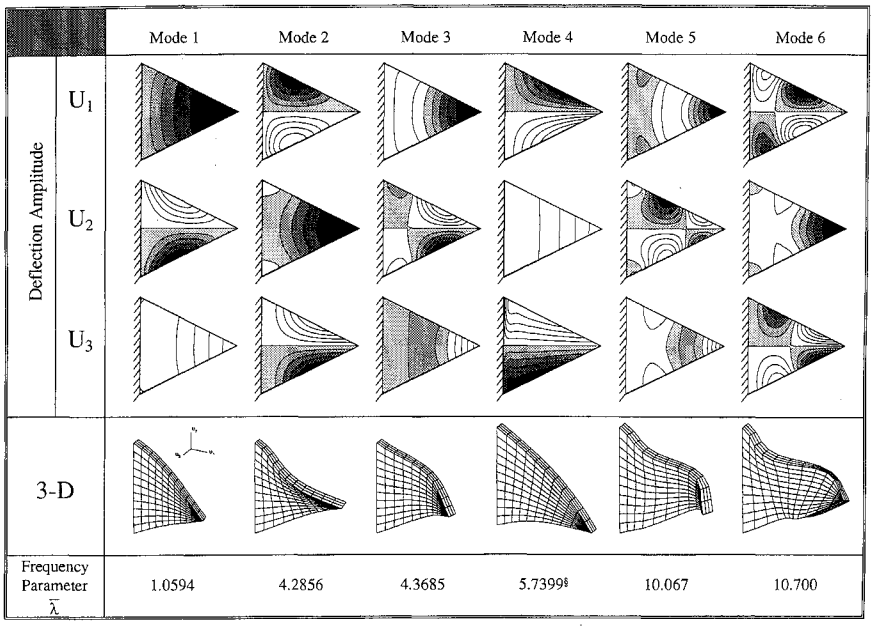

Fig. 2a Three-dimensional vibration mode shapes for the cantilevered isosceles triangular plate with $a/b = 1.0$, $t/b = 0.1$, $\theta = \tan^{-1}(1/2)$, and $\nu = 0.3$ (§ denotes symmetric thickness mode).

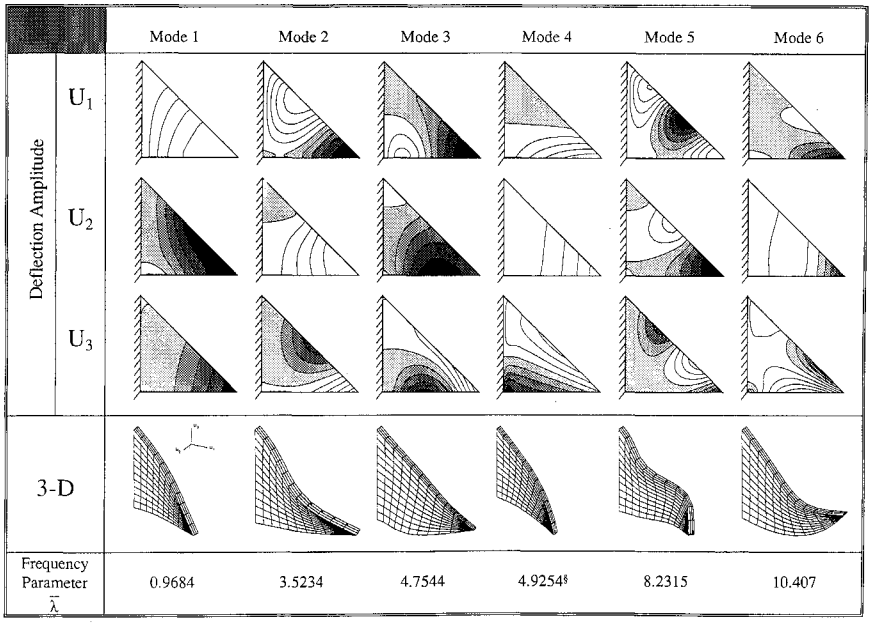

Fig. 2b Three-dimensional vibration mode shapes for the cantilevered right angle triangular plate with $a/b = 1.0$, $t/b = 0.1$, $\theta = 0$ deg, and $\nu = 0.3$ (§ denotes symmetric thickness mode).

For the remaining edges, the following stress-free conditions hold:

$$\sigma_{ij} = 0, \quad i, j = 1, 2, 3 \tag{22}$$

The basic surface functions that satisfy concurrently the essential boundary conditions implied in Eqs. (21) and (22) are, respectively,

$${}^{i}\phi_1(x_1, x_2) = (x_1 + a/2), \quad i = 1, 2, 3 \tag{23}$$

B. Derivation of Governing Eigenvalue Equation

Substituting the displacement amplitude functions defined in the preceding sections into Eq. (10) and minimizing with respect to the unknown coefficients according to the Ritz procedure,

$$\frac{\partial \Pi}{\partial C_{mn}^{i}} = 0; \quad i = 1, 2, \text{and } 3 \tag{24}$$

we obtain a set of linear eigenvalue equations for the vibration frequencies and mode shapes of the skewed trapezoidal plate:

$$(\boldsymbol{K} - \Omega^2 \boldsymbol{M})\{\boldsymbol{C}\} = \{0\} \tag{25}$$

where $\boldsymbol{K}$ and $\boldsymbol{M}$ are the generalized stiffness and consistent mass matrices of the skew trapezoidal plate, respectively,

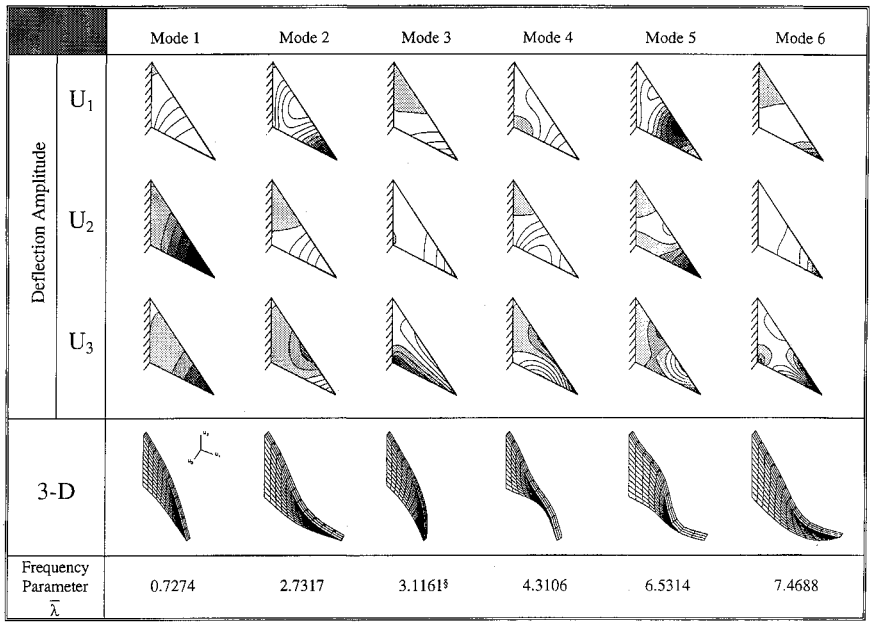

Fig. 2c Three-dimensional vibration mode shapes for the cantilevered skewed triangular plate with $a/b = 1.0$, $t/b = 0.1$, $\theta = -\tan^{-1}(1/2)$, and $\nu = 0.3$ (§ denotes symmetric thickness mode).

$$\boldsymbol{K} = \begin{bmatrix} \boldsymbol{k}^{11} & \boldsymbol{k}^{12} & \boldsymbol{k}^{13} \\ & \boldsymbol{k}^{22} & \boldsymbol{k}^{23} \\ \text{sym} & & \boldsymbol{k}^{33} \end{bmatrix} \tag{26a}$$

$$\boldsymbol{M} = \begin{bmatrix} \boldsymbol{m}^{11} & 0 & 0 \\ & \boldsymbol{m}^{22} & 0 \\ \text{sym} & & \boldsymbol{m}^{33} \end{bmatrix} \tag{26b}$$

and $\{\boldsymbol{C}\} = \{C^1_{mn}, C^2_{mn}, C^3_{mn}\}^T$ is the column vector of the unknown coefficients.

The elements in the stiffness matrix $\boldsymbol{k}^{\alpha\beta}$ are given by

$$k^{11}_{mjnk} = \frac{1-\nu}{(1-2\nu)}(E^{1010}_{mj}F^{00}_{nk})_{11} + \frac{1}{2}\left[\left(\frac{a}{b}\right)^2 (E^{0101}_{mj}F^{00}_{nk})_{11} + \left(\frac{a}{t}\right)^2 (E^{0000}_{mj}F^{11}_{nk})_{11}\right] \tag{27a}$$

$$k^{12}_{mjnk} = \left(\frac{a}{b}\right)\left[\frac{\nu}{(1-2\nu)}(E^{1001}_{mj}F^{00}_{nk})_{12} + \frac{1}{2}(E^{0110}_{mj}F^{00}_{nk})_{12}\right] \tag{27b}$$

$$k^{13}_{mjnk} = \left(\frac{a}{t}\right)\left[\frac{\nu}{(1-2\nu)}(E^{1000}_{mj}F^{01}_{nk})_{13} + \frac{1}{2}(E^{0010}_{mj}F^{10}_{nk})_{13}\right] \tag{27c}$$

$$k^{22}_{mjnk} = \left(\frac{a}{b}\right)^2 \frac{1-\nu}{(1-2\nu)}(E^{0101}_{mj}F^{00}_{nk})_{22} + \frac{1}{2}\left[(E^{1010}_{mj}F^{00}_{nk})_{22} + \left(\frac{a}{t}\right)^2 (E^{0000}_{mj}F^{11}_{nk})_{22}\right] \tag{27d}$$

$$k^{23}_{mjnk} = \left(\frac{a^2}{bt}\right)\left[\frac{\nu}{(1-2\nu)}(E^{0100}_{mj}F^{01}_{nk})_{23} + \frac{1}{2}(E^{0001}_{mj}F^{10}_{nk})_{23}\right] \tag{27e}$$

$$k^{33}_{mjnk} = \left(\frac{a}{t}\right)^2 \frac{1-\nu}{(1-2\nu)}(E^{0000}_{mj}F^{11}_{nk})_{33} + \frac{1}{2}\left[\left(\frac{a}{b}\right)^2 (E^{0101}_{mj}F^{00}_{nk})_{33} + (E^{1010}_{mj}F^{00}_{nk})_{33}\right] \tag{27f}$$

and the explicit expressions for the mass matrix $\boldsymbol{m}^{\alpha\beta}$ are given by

$$m^{11}_{mjnk} = (1+\nu)(E^{0000}_{mj}F^{00}_{nk})_{11} \tag{27g}$$

$$m^{22}_{mjnk} = (1+\nu)(E^{0000}_{mj}F^{00}_{nk})_{22} \tag{27h}$$

$$m^{33}_{mjnk} = (1+\nu)(E^{0000}_{mj}F^{00}_{nk})_{33} \tag{27i}$$

where

$$(E^{defg}_{mj})_{\alpha\beta} = \int_{-0.5}^{0.5}\int_{-0.5}^{0.5} \left\{\frac{\partial^{d+e}[{}^{\alpha}\phi_m(\bar{x}_1,\bar{x}_2)]}{\partial\bar{x}_1^d\partial\bar{x}_2^e}\right\}\left\{\frac{\partial^{f+g}[{}^{\beta}\phi_j(\bar{x}_1,\bar{x}_2)]}{\partial\bar{x}_1^f\partial\bar{x}_2^g}\right\} d\bar{x}_1\, d\bar{x}_2 \tag{28a}$$

$$(F^{rs}_{nk})_{\alpha\beta} = \int_{-0.5}^{0.5} \left\{\frac{\partial^r[{}^{\alpha}\psi_n(\bar{x}_3)]}{\partial\bar{x}_3^r}\right\}\left\{\frac{\partial^s[{}^{\beta}\psi_k(\bar{x}_3)]}{\partial\bar{x}_3^s}\right\} d\bar{x}_3 \tag{28b}$$

in which $\alpha, \beta = 1, 2, 3$ and the variables $\bar{x}_1$, $\bar{x}_2$, and $\bar{x}_3$ in the preceding integrations are defined in the nondimensionalized forms as

$$\bar{x} = \frac{x_1}{a}; \quad \bar{x}_2 = \frac{x_2}{b} \text{ and } \bar{x}_3 = \frac{x_3}{t} \tag{29}$$

Finally, solving for the eigenvalue defined in Eq. (25) yields

$$\Omega = \omega a\sqrt{\rho/E} \tag{30}$$

IV. Numerical Studies

The global three-dimensional elasticity formulation developed in the preceding section is now applied to the vibration analysis of cantilevered skewed trapezoidal plates. Frequency results computed are expressed in the nondimensional form as

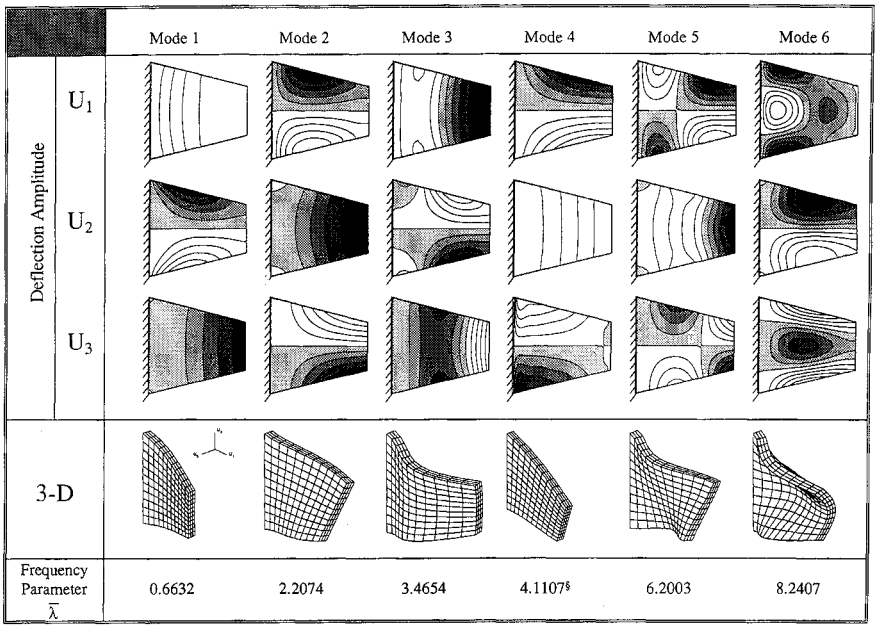

Fig. 3a Three-dimensional vibration mode shapes for the cantilevered trapezoidal plate with $a/b = 1.0$, $c/b = 0.5$, $t/b = 0.1$, $\theta = \tan^{-1}(1/4)$, and $\nu = 0.3$ (§ denotes symmetric thickness mode).

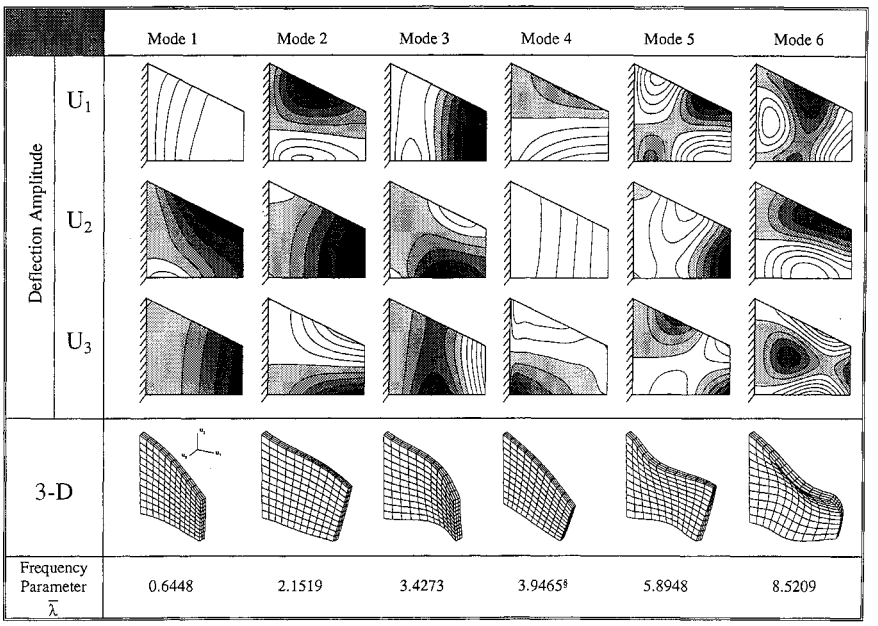

Fig. 3b Three-dimensional vibration mode shapes for the cantilevered trapezoidal plate with $a/b = 1.0$, $c/b = 0.5$, $t/b = 0.1$, $\theta = 0$ deg, and $\nu = 0.3$ (§ denotes symmetric thickness mode).

$$\bar{\lambda} = (\omega b^2/2\pi)\,(\rho t/D)^{1/2} \tag{31}$$

Cantilevered trapezoidal plates having different skew angles, aspect ratios, and chord ratios were examined in the present work. Plates with thickness ratios ranging from the limits of classical thin plates to very thick solid prisms were considered. The accuracy of the proposed formulation is established through extensive convergence studies and comparison with the existing analytical and experimental results.

A. Convergence and Comparison Studies

Convergence studies have been carried out for cantilevered trapezoidal plates of different aspect ratio, degree of skewness, and chord ratio. The convergence patterns for plates in the form of isosceles triangles and symmetric trapezoids are shown in Table 1. The degree p of the polynomial for the surface function and the number of terms q for the thickness function are varied in different steps to show their relative effects on the overall convergence behavior. In this study, equal numbers of terms are assumed for the displacement components in U_1, U_2, and U_3. The thickness ratios are taken to be 0.01 and 0.1.

In general, it is observed that the present three-dimensional Ritz solutions converge monotonically from above to the frequency values. From Table 1, it is further noticed that the rate of convergence for the first six frequency parameters is more sensitive to the order p of the polynomial employed in the surface function than that of the number of terms q used in the thickness direction. In

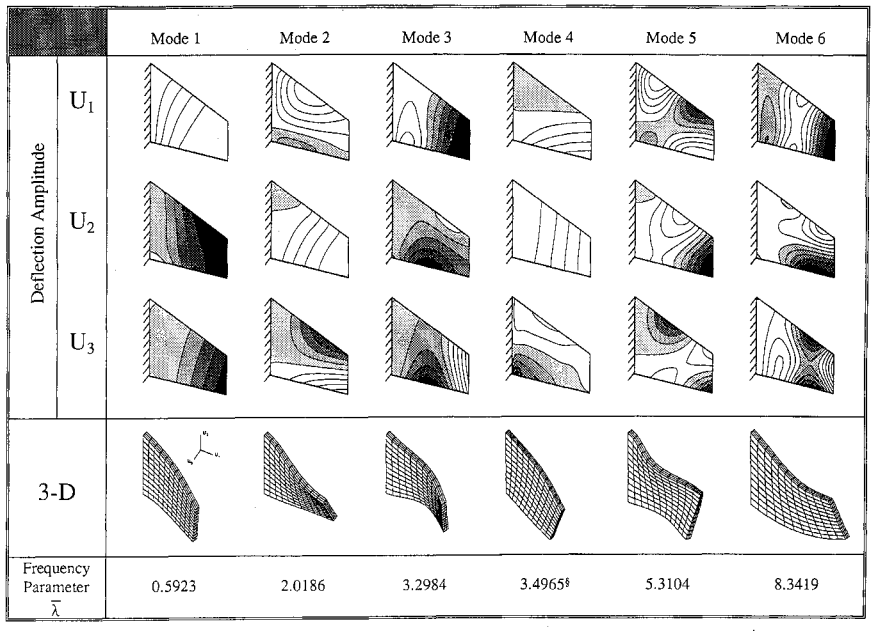

Fig. 3c Three-dimensional vibration mode shapes for the cantilevered trapezoidal plate with $a/b = 1.0$, $c/b = 0.5$, $t/b = 0.1$, $\theta = -\tan^{-1}(1/4)$, and $\nu = 0.3$ (§ denotes symmetric thickness mode).

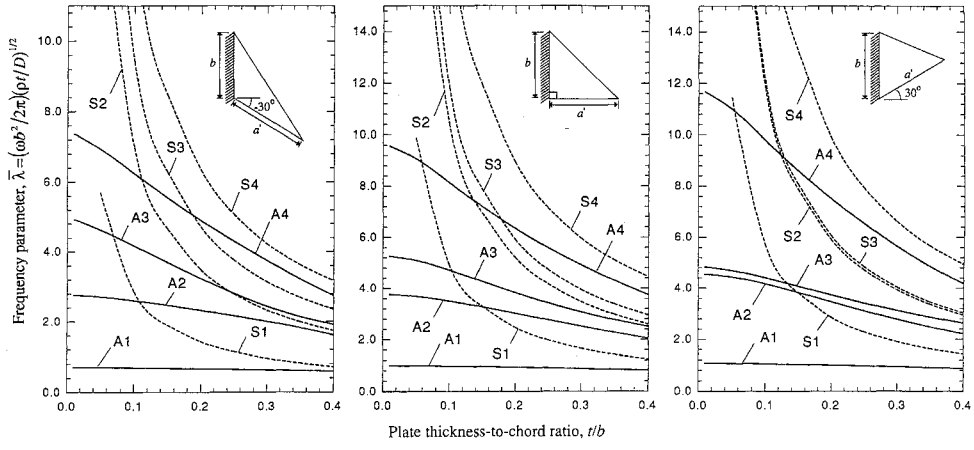

Fig. 4 Plots of frequency parameters $\bar{\lambda}$ vs thickness ratio t/b for cantilevered skewed triangular plates at different skew angles with $\nu = 0.3$ and $a'/b = 1/\cos\theta$ [---, symmetric thickness modes (S) and —, antisymmetric thickness modes (A)].

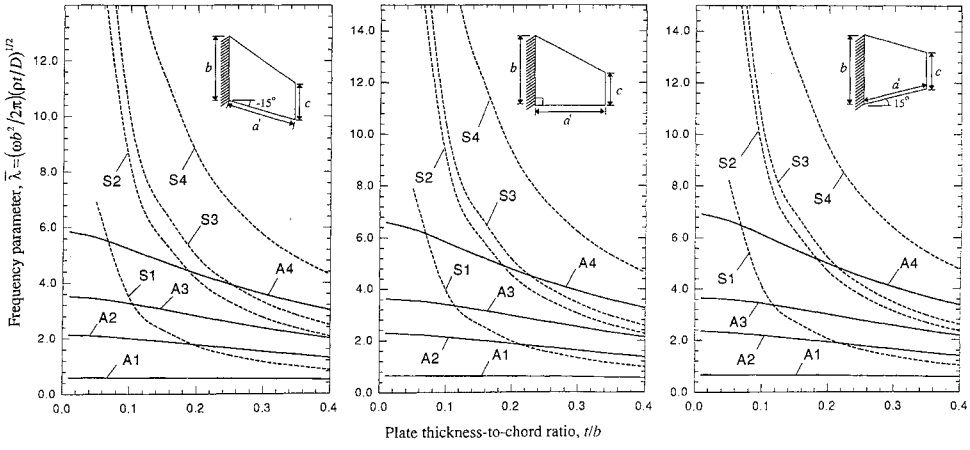

Fig. 5 Plots of frequency parameters $\bar{\lambda}$ vs thickness ratio t/b for cantilevered skewed trapezoidal plates at different skew angles with $\nu = 0.3$, $a'/b = 1/\cos\theta$, and $c/b = 0.5$ [---, symmetric thickness modes (S) and —, antisymmetric thickness modes (A)].

other words, significant improvement in the solutions can be attained merely by employing a higher-order polynomial in the surface direction while keeping relatively low terms of thickness function. Moreover, from the convergence studies, it is observed that the present solutions converged faster for plates with higher thickness ratios. For the triangular plate with thickness ratio of 0.01, for instance, the eigenvalues computed using 13×5 terms are within 0.02% of the corresponding eigenvalues computed using 12×5 terms. Similar accuracy is achieved for a thick plate ($t/b = 0.10$) with 11×5 terms in the deflection series. From the convergence studies presented, it was decided that 12×5 terms should be used in the present study to retain accurate frequency parameters at a reasonable computation cost.

Having established the number of terms needed in the deflection series for reasonably converged solutions, the accuracy of the frequency results are validated through comparison with the existing analytical and experimental data. For thin, unsymmetric trapezoidal plates, the computed frequency parameters are compared in Table 2 with the two-dimensional finite element solutions of Mirza and Bijlani[1] and the analytical results of McGee et al.[3] who use corner stress functions for the treatment of stress singularities. For the special case of a delta (or right angle triangular) plate, the experimental results of Gustafson et al.[12] are included. It is noted that the present three-dimensional Ritz solutions compared quite favorably with the analytical results. On the other hand, the experimental values for the delta triangular plate are lower although of the same order of magnitude.

The frequency results for cantilevered isosceles triangular plates are presented in Table 3 together with the classical plate solutions of Bhat[2] for the special case of a thin equilateral triangular plate and the Mindlin plate solutions of Kitipornchai et al.[4] For thin triangular plates, the results from the classical thin plate theory, the Mindlin shear deformable plate theory, and the present three-dimensional Ritz method are found to be in good agreement. This is because for the thin plate ($t/b \leq 0.01$) the effects of shear deformation and rotary inertia are negligible. For the moderately thick plate, the Mindlin formulation of Ref. 4, which uses a shear correction factor $\kappa = 5/6$, tends to give a lower frequency. It is further noticed that the present three-dimensional Ritz method is able to represent more modes than the Mindlin plate solutions. For instance, for the equilateral triangular thick plate ($\theta = 30$ deg and $t/b = 0.1$), the three-dimensional Ritz method yields two symmetric thickness modes at $\bar{\lambda} = 7.0541$ and 13.772 in addition to the first six modes predicted in the Mindlin formulation. Table 4 presents the frequency parameters computed for the cantilevered symmetric trapezoidal plates. The Mindlin solutions by Kitipornchai et al.[5] are listed for comparison. Again it is observed that for thin plates both methods yield comparable frequencies for plates of different aspect ratios and chord ratios. However, as the plate thickness increases, the Mindlin solutions tend to give lower values as compared with the present three-dimensional Ritz solutions. In addition, the present three-dimensional Ritz formulation, by virtue of its exact derivation from the three-dimensional elasticity theory that allows for the higher-order thickness variation, is able to identify the symmetric thickness modes that are absent in the Mindlin solutions.

B. Natural Modes of Vibration

In this section, the proposed three-dimensional Ritz formulation is applied to compute the natural mode of vibration for moderately thick skewed trapezoidal plates. Values of the nondimensional frequency parameters $\bar{\lambda}$ and the corresponding three-dimensional deformed mode shapes are presented in Figs. 2a–2c for cantilevered skewed triangular plates. In Figs. 3a–3c the vibration mode shapes for cantilevered skewed trapezoidal plates having $c/b = 0.5$ are shown. The aspect ratio a/b and the thickness ratio t/b are fixed at 1.0 and 0.1, respectively.

For the isosceles triangular plate shown in Fig. 2a, it is observed that the vibration motions at the first, third, and fifth modes are predominantly spanwise bending modes. On the other hand, torsional motions can be identified at the second and the sixth modes of vibration. At the fourth mode, the plate exhibits pure surface

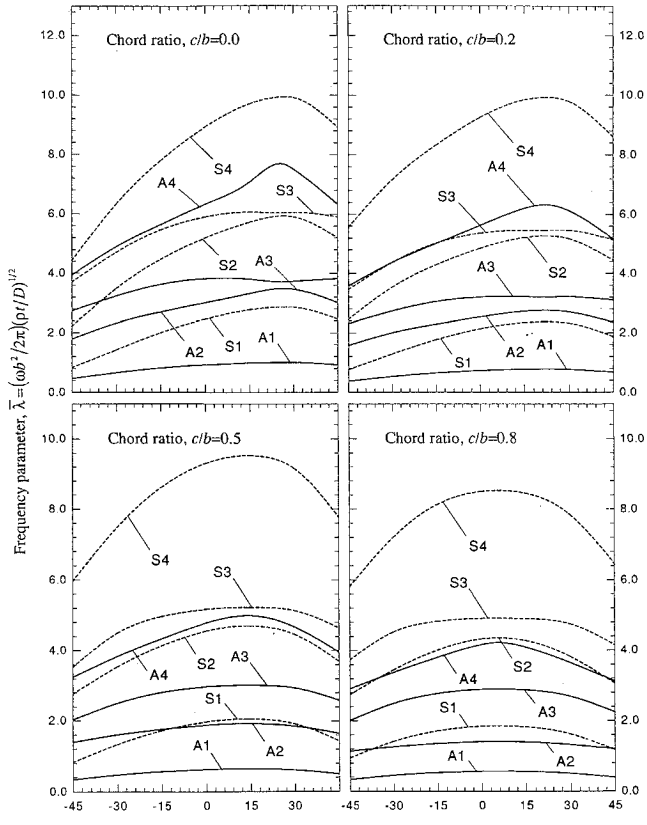

Fig. 6 Plots of frequency parameters $\bar{\lambda}$ vs skew angle θ for cantilevered thick skewed trapezoidal plates at different chord ratios with ν = 0.3, a'/b = 1/cos θ, and t/b = 0.2 [---, symmetric thickness modes (S) and —, antisymmetric thickness modes (A)].

parallel motion (which is the first symmetric thickness mode). These modes are also found in triangular plates having different degrees of skewness as shown in Figs. 2b and 2c. However, in these configurations, coupling between the spanwise bending and the torsional motions becomes more significant (for instance, in the second and the third modes of the right angle triangular plate).

The vibration characteristics of the cantilevered skewed trapezoidal plates can be clarified by considering the deformed mode shapes depicted in Figs. 3a–3c. These can be characterized as spanwise bending, torsion, and surface parallel motions. The corresponding eigenvalues at each mode of vibration are presented below the three-dimensional deformed geometry diagrams. It is worth noting that for both skewed triangular and trapezoidal plates, as the degree of skewness changes from positive to negative, the nondimensional frequency parameter $\bar{\lambda}$ tends to decrease monotonically. To further quantify the relative effects of the geometric parameters on the vibration response of these plates, a more thorough parametric study is carried out and discussed in the following section.

C. Influence of Geometric Parameters

The plots of frequency parameters $\bar{\lambda}$ vs the thickness ratios for cantilevered skewed triangular and trapezoidal plates are presented in Figs. 4 and 5. The skew angles were fixed at −30, 0, and 30 deg for the triangular planform and at −15, 0, and 15 deg for the trapezoidal planform, respectively. Two sets of curves, each corresponding to modes having symmetric and antisymmetic thickness variations, are presented in these plots. For thin plates ($t/b \leq 0.01$), it is found that the lower vibration spectrum is dominated by antisymmetric thickness modes. These modes exhibit predominantly spanwise bending, torsion, and chordwise bending motions. It is interesting to note that as the thickness ratio increases, the symmetric thickness modes (which are predominantly the surface parallel modes) began to dominate the lower frequency spectrum. The points of intersection between these two sets of curves are

identified as modes having strong coupling between these two distinct symmetry classes of vibration.

To investigate the effects of plate skewness on the frequency response of thick skewed triangular and trapezoidal plates (with thickness ratio, $t/b = 0.2$), graphs of frequency parameters vs the degrees of skewness are computed (as shown in Fig. 6). The degrees of skewness range from −45 to 45 deg, and the chord ratio c/b varies from 0.0 to 0.8 in these plots. Frequency parameters that correspond to the first six modes of each symmetry class about the thickness are presented. It is noted that, for thick trapezoidal plates of constant chord ratio c/b, the degree of skewness has initially a stiffening effect on the overall vibration response. However, as the skew angle increases further, the frequency parameters decrease in a symmetric manner. An examination of these plots further reveals that, for trapezoidal plates having the same skew angle, the frequency parameters tend to decrease with the chord ratio c/b. The presence of both the symmetric and antisymmetric thickness modes in the lower vibration spectrum are also observable in these plots.

V. Conclusions

This paper describes the detailed development of a global three-dimensional Ritz formulation for the free vibration analysis of plates. The method is applied in the present work to compute the vibration frequencies and mode shapes of cantilevered skewed trapezoidal plates of arbitrary planform. It is demonstrated through vivid three-dimensional deformed mode shape plots and comprehensive parametric studies that the present approach can provide a full vibration spectrum for the analysis of these structures. Notable is the extraction of several modes having symmetric thickness variations. These modes are found to be absent in the conventional two-dimensional method of analysis.

In addition, through the parametric studies, some important conclusions relating to the design of these structures have been deduced. It was found that an increase in the frequency parameters is brought about by a corresponding decrease in the chord ratio. Plates with higher thickness ratios are also found to possess lower frequency parameters.

References

[1]Mirza, S., and Bijlani, M., "Vibration of Triangular Plates of Variable Thickness," *Computers and Structures*, Vol. 21, No. 6, 1985, pp. 1129–1135.

[2]Bhat, R. B., "Flexural Vibration of Polygonal Plates Using Characteristics Orthogonal Polynomials in Two Variables," *Journal of Sound and Vibration*, Vol. 114, No. 1, 1987, pp. 65–71.

[3]McGee, O. G., Leissa, A. W., and Huang, C. S., "Vibrations of Cantilevered Skewed Trapezoidal and Triangular Plates with Corner Stress Singularities," *International Journal of Mechanical Sciences*, Vol. 34, No. 1, 1992, pp. 63–84.

[4]Kitipornchai, S., Liew, K. M., Xiang, Y., and Wang, C. W., "Free Vibration of Isosceles Triangular Mindlin Plates," *International Journal of Mechanical Sciences*, Vol. 35, No. 2, 1993, pp. 89–102.

[5]Kitipornchai, S., Xiang, Y., Liew, K. M., and Lim, M. K., "A Global Approach for Vibration of Thick Trapezoidal Plates," *Computers and Structures*, 1994 (to be published).

[6]Mindlin, R. D., "Influence of Rotary Inertia and Shear in Flexural Motion of Isotropic, Elastic Plates," *ASME Journal of Applied Mechanics*, Vol. 18, March 1951, pp. 1031–1036.

[7]Srinivas, S., Rao, C. V. J., and Rao, A. K., "An Exact Analysis for Vibration of Simply Supported Homogeneous and Laminated Thick Rectangular Plates," *Journal of Sound and Vibration*, Vol. 12, No. 2, 1970, pp. 187–199.

[8]Liew, K. M., Hung, K. C., and Lim, M. K., "A Continuum Three-Dimensional Vibration Analysis of Thick Rectangular Plates," *International Journal of Solids and Structures*, Vol. 30, No. 24, 1993, pp. 3357–3379.

[9]Lam, K. Y., and Hung, K. C., "Orthogonal Polynomials and Subsectioning Method for Vibration of Plates," *Computers and Structures*, Vol. 34, No. 6, 1990, pp. 827–834.

[10]Liew, K. M., "The Development of 2-D Orthogonal Polynomials for Vibration of Plates," Ph.D. Thesis, Dept. of Mechanical and Production Engineering, National Univ. of Singapore, 1990.

[11]Chihara, T.S., *An Introduction to Orthogonal Polynomials*, Gordon & Breach, New York, 1978.

[12]Gustafson, P. N., Stokey, W. F., and Zorowski, C. F., "An Experimental Study of Natural Vibrations of Cantilevered Triangular Plates," *Journal of Aerospace Sciences*, Vol. 20, 1953, pp. 331–337.